3rd URSI AT-AP-RASC, Gran Canaria, 29 May – 3 June 2022

First Morphological Results of the GPS L-band Amplitude Scintillation from Tarawa Equatorial Station

Sarvesh Kumar * (1), Sushil Kumar (2)
School of Information Technology, Engineering, Mathematics and Physics
The University of the South Pacific, Suva, Fiji. https://www.usp.ac.fj/

Abstract

We present the first morphological results of the Global Positioning Systems (GPS) L_1 and L_2 band amplitude scintillation (S_4 index) from Tarawa Equatorial Station (geog: 1.33°N, 173.01°E, geomag: 2.68°S, 114.26°W). The analysis period of September 2017 to November 2018 falls in the low solar activity period of solar cycle 24 (avg sunspot# = 11.6). The scintillation data were analyzed to study the diurnal variation, seasonal variation, geomagnetic dependence, and solar flare dependence of the S_4 index. No daytime scintillations were observed during the entire study period on either of the bands. Nighttime scintillations had maximum occurrence during equinox months followed by summer and then winter. L_2 band recordings showed an increased level of scintillation compared to the L_1 band. Geomagnetic disturbances effect showed increased scintillation activities during the magnetically disturbed days compared to quiet days. Scintillations during geomagnetic storms were dominantly confined in the pre-midnight hours and finally, scintillations were found to be completely absent during solar flare events. **Note: Some figures are not shown in this summary paper due to page limit.**

1. Introduction

Satellite transionospheric communication is a heavily used method in the fields of navigation, military application, communication, and ionospheric research. The satellites of the Global Positioning System (GPS) constellation transmit at 3 different frequencies; L_1 (1575.42 MHz), L_2 (1227.6 MHz), and L_5 (1176 MHz). As the signals propagate through the ionosphere, it undergoes scattering and rapid modification due to the small-scale structures in the ionosphere known as irregularities in a process called scintillation. Scintillation can be quantified by the S_4 index which measures the fluctuations in the amplitude of the signals. Scintillation can be disastrous to GPS users causing problems such as larger positioning errors and loss of signal lock on the receivers.

The equatorial night-time scintillations occur due to generalized Rayleigh-Taylor instability (GRT instability) and Pre-Reversal Enhancement (PRE) [1-4] which creates Equatorial Plasma Bubbles (EPB) and ionospheric instabilities at the magnetic equator (known as Equatorial Spread F (ESF)) which forms under the F-region [5-8]. With sunset, the ionization energy also decreases and as a result, the electron density of the ionosphere becomes less. The decrease in E-region electron density and the interaction with the atmospheric neutral wind (i.e. the ion-neutral collision) generates an enhanced eastward electric field known as PRE on the dayside of the sunset and westward electric field on the night side of the sunset [9]. This causes a brief but intense uplifting of the plasma triggering a height increase in the ionosphere due to **E×B** (equatorial fountain effect, EFE). The PRE disturbs the ionosphere and causes steep electron density gradients on the bottom side of the F-region [5] and as a result, a rapid GRT instability occurs[10]. GRT instability tries to bring the ionosphere back to equilibrium thus the regions of different densities start to move. The lower density region (or bubbles/EPBs) moves up through the ionosphere to settle on the topside. The instability starts as a large structure and gets divided into smaller cascade structures as they move through the ionosphere[9-11]. Once these structures reach the maximum height, they diffuse at locations off the magnetic equator around approximately ± 20° north and south to form the region which is known as the Equatorial Ionization Anomaly (EIA) [3, 11-13]. It is due to these structures along the different altitudes of the ionosphere which causes the L band scintillations. Day-time scintillations, however, have been attributed to E-region irregularities often referred to as Sporadic-E (Es) [14]) (or Equatorial Sporadic-E (Esq)) which forms during the day and has a higher chance of forming just after sunrise with some assistance provided by the gravity waves [15-17].

There have been studies on the GPS L_1 band scintillations in the Pacific Region [16, 18], however, from our literature review, no focus was made on the L_2 band in this region. Additionally, these studies only focused on the crest of the EIA regions. In this study, we present the first results from Tarawa which is in the trough of the EIA region with a focus on both, the L_1 and L_2 band scintillation.

2. Method

The S_4 data on GPS L_1 and L_2 bands were recorded using a Septentrio PolaRx5S receiver which was installed at The

University of the South Pacific Campus in Tarawa, Kiribati (geographic coordinates: 1.33°N, 173.01°E, geomagnetic coordinates: 2.68°S, 114.26°W) in September 2017. The data from September 2017 to November 2018 has been used for this study.

S_4 is recorded by the receiver as the standard deviation of 50 Hz raw signal power normalized to the average signal power over a one-minute interval as S_{4total}. The receiver also outputs the correction due to thermal noise on S_{4total} as S_{4cor} thus the final S_4 which can be used for analysis is given by:

$$S_{4_{final}} = \sqrt{S4_{total} - S4_{cor}} \qquad (1.0)$$

If $S_{4cor} > S_{4total}$ Then $S_{4final} = 0$

A classification of S_4 according to its strength used by Prasad et al. (2016) was adopted for this study to classify S_4 as very weak, weak, moderate, and strong.

Table 1.0: S_4 classification by Prasad et al. (2016).

***S*₄ Strength**	***S*₄ value (unitless)**
Very weak	$0.17 \leq S_4 < 0.2$
Weak	$0.2 \leq S_4 < 0.3$
Moderate	$0.3 \leq S_4 < 0.45$
Strong	$0.45 \leq S_4$

All $S_4 < 0.17$ were regarded as noise.

The minute average of S_{4final} (from here on referred to as only S_4) was calculated. To qualify as a scintillation, an event had to fall into one of the categories of Table 1.0 and should have lasted for at least 3 minutes. The S_4 with the largest value in 15-minute intervals was identified and using the above two criteria, the data from the station were analyzed using two variables- the number of scintillation events and the %occurrence of scintillation events. S_4 variations were then analyzed under different conditions such as diurnal, seasonal, annual, geomagnetic disturbance (using the international geomagnetic quiet and disturbed days), geomagnetic storms, and solar flare effects.

3. Results and Discussion

3.1 Diurnal, Seasonal and Annual Variation of Scintillation

Scintillation activity at Tarawa on both bands initiated after 18:00 LT and slowly increased until approx. 20:00 LT after which a very sharp increase in the percentage occurrence of S_4 index is seen reaching a max of 0.9% on L_1 and 1.7% on L_2 (Figure 1.0 a, b). These peaks appear at midnight after which the scintillation activity decreases. Scintillation on L_1 decreases more rapidly as compared to the L_2 band and reaches zero percent after approximately 2:00 LT. Scintillation activity at Tarawa was seen to be a total nighttime phenomena during this study period.

The occurrence of diurnal patterns of scintillation at our stations can be attributed to the development of F-region irregularities (equatorial spread F) forming after sunset due to PRE creating GRT instabilities [19, 20] which is responsible for the creation of equatorial plasma bubbles needed for scintillation to occur.

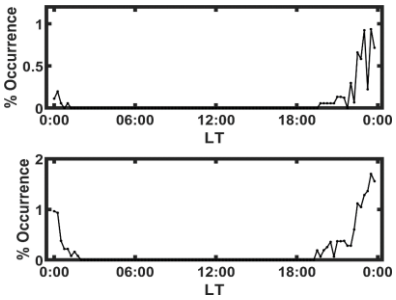

Figure 1.0: Diurnal annual average percentage occurrence of GPS (a) L_1 band and (b) L_2 band scintillations at Tarawa September 2017- November 2018.

To study the seasonal variation (figure not shown), S_4 data were grouped into Summer, Winter, and Equinox months. Scintillation in the equinox was the most dominant on both bands followed by summer and then winter. The most dominant category of scintillation was weak scintillations followed by very weak, moderate, and then strong. The L_2 band recorded 300% more events in summer and 290.2% more events in equinox as compared to the L_1 band.

Equatorial plasma bubbles and equatorial spread F occurrence have been directly correlated with the solar activity and shown to increase during equinoctial months [20]. Similarly, the large magnetic declination angle over the equatorial region, with good alignment between the sunset terminator and the magnetic meridian around the equinox months has also been attributed to the increased rate and strength of the L band scintillations [20, 21].

In figure 2.0 (Figure not shown here) it is seen that the station recorded no daytime scintillation event throughout the recording period. The figure also shows that scintillation activity was dominantly a pre-midnight phenomenon throughout the year. Annually (Figure 3.0 a, b), the L_2 band signal showed 292.9% more scintillation events than the L_1 band signal. The L_2 band signal is also seen to be more susceptible to moderate and strong scintillation activities ($S_4 >= 0.30$) as compared to the L_1 band signal since L_1 did not record any strong events ($S_4 > 0.45$).

The observation of increased scintillation on the lower frequency band at Tarawa is indicative of the frequency dependence relationship of S_4 i.e. $S_4 \propto f^{-n}$ where $n \approx 1.5$ for $S4 < 0.6$ and $S4 > 0.6$, n decreases monotonically [22, 23].

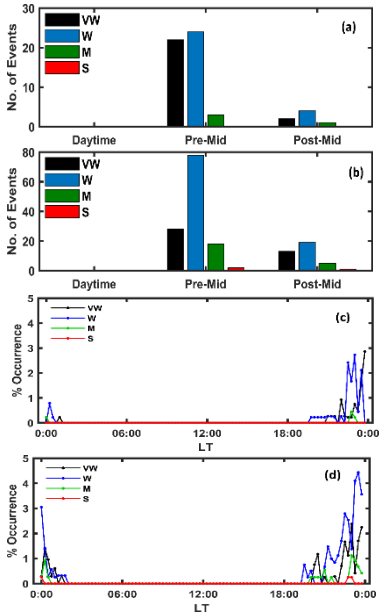

Figure 3.0 (a-d): Annual analysis of the number of scintillation events on GPS (a) L_1 band, (b) L_2 band, and the diurnal percentage occurrence of scintillation on (c) L_1 band and (d) L_2 band at Tarawa from September 2017 to November 2018. The strength of scintillations (S_4) is represented by the colored bars; VW-very weak ($0.17 \leq S_4 < 0.2$), W-weak ($0.2 \leq S_4 < 0.3$), M-moderate ($0.3 \leq S_4 < 0.45$) and S-strong ($0.45 \leq S_4$).

3.2 Geomagnetic Disturbance, Geomagnetic Storm and Solar Flare Effect on Scintillation

The geomagnetic disturbance effect was studied by looking at the S_4 variations during the 5 international geomagnetically quiet (Q) and disturbed (D) days for both bands (figure not shown). D days recorded a total of 27 events and Q days recorded 12 events showing higher activity (nearly 70% increase) on D days compared to Q days on the L_1 band. For L_2 band, the disturbed period showed 56 scintillation events while the quiet period recorded 24 events. L_2 band also showed a 70% increase in the occurrence of scintillation events during the disturbed period.

To study the geomagnetic storm effect on scintillation, storms with Dst < -50nT were considered and the scintillation activity during these storms are summarised in Table 2.0:

Table 2.0. A summary of scintillation occurrence during geomagnetic storm events. The table summarizes the minimum Dst index of the storm, local time (LT) occurrence of the different steps of the storm, type of storm (SSC- sudden storm commencement or SGC- Storm gradual Commencement) and the local time of scintillation occurrence during the initial, main and recovery phases of the geomagnetic storm.

#	Min *Dst*	LT of Step 1	LT of Step 2	Type	Season	Initial	Main	Recovery
1	-124	8/9/2017 13:00	9/9/2017 5:00	SSC	E	Pre_mid night	-	Pre_mid night
2	-55	28/9/2017 18:00		SGC	E	Pre_mid night	Pre_mid night	No data
3	-74	7/11/2017 19:00	8/11/2017 13:00	SGC	W	-	-	Pre_mid night
4	-66	20/4/2018 21:00	21/4/2018 6:00	SSC	E	Pre_mid night	-	Pre_mid
5	-56	6/5/2018 6:00	6/5/2018 14:00	SSC	S	Pre_mid night		Pre_mid night
6	-174	26/8/2018 19:00		SGC	S	-	Pre_mid night	-
7	-60	11/9/2018 11:00	11/9/2018 22:00	SGC	E	-	-	-

A unique observation from this analysis was that all storms only produced scintillations in the local pre-midnight hours with no daytime or post-midnight scintillation. Another observation was that scintillation during the main phase was relatively less (2 events) when compared to the initial and recovery phases of the storm (4 events each). These two observations are indicative of a strong dependence of scintillation on the PRE of the vertical **E × B** drift due to the eastward electric field at the magnetic equator as it only occurs with sunset [24, 25], in our case, even during geomagnetic storms.

A similar analysis was also carried out for solar flares (table not shown). However, it was earlier established that the scintillation events at Tarawa were only a nighttime feature and since solar flares are mostly seen to produce ionospheric effects in the dayside, it was found that scintillation during the flares was completely absent.

4. Conclusion

The scintillation activity at the equator was found to be short-lived (approximately 6 hrs) and only occurred in the nighttime of the study period. Scintillation in the equinox was the most dominant with scintillation on the L_2 band being dominant throughout the study period. A strong dependence of scintillation occurrence on geomagnetic disturbance was seen, however, it was unique to see that all geomagnetic storms only produced scintillation in the pre-midnight hours. No relationship was found between solar flares and scintillation activity. Generally, scintillation activity at Tarawa is suggested to be caused by equatorial spread F due to pre-reversal enhancement, development of ionospheric irregularities and equatorial plasma bubbles in the post-sunset hours.

5. References

[1] A. DasGupta, A. Maitra, and S. Das, "Post-midnight equatorial scintillation activity in relation to geomagnetic disturbances," *Journal of atmospheric and terrestrial physics*, vol. 47, no. 8-10, pp. 911-916, 1985, doi: 10.1016/0021-9169(85)90067-4.

[2] J. V. Eccles, "Modeling investigation of the evening prereversal enhancement of the zonal electric field in the equatorial ionosphere," *Journal of Geophysical Research: Space Physics*, vol. 103, no. A11, pp. 26709-26719, 1998, doi: 10.1029/98JA02656.

[3] B. G. Fejer, D. Farley, R. Woodman, and C. Calderon, "Dependence of equatorial F region vertical drifts on

season and solar cycle," *Journal of Geophysical Research: Space Physics*, vol. 84, no. A10, pp. 5792-5796, 1979, doi: 10.1029/JA084iA10p05792.

[4] Y. Jiao and Y. T. Morton, "Comparison of the effect of high-latitude and equatorial ionospheric scintillation on GPS signals during the maximum of solar cycle 24," *Radio Science*, vol. 50, no. 9, pp. 886-903, 2015, doi: 10.1002/2015RS005719.

[5] J. Aarons, J. Klobuchar, H. Whitney, J. Austen, A. Johnson, and C. Rino, "Gigahertz scintillations associated with equatorial patches," *Radio Science*, vol. 18, no. 03, pp. 421-434, 1983, doi: 10.1029/RS018i003p00421.

[6] D. Farley, B. Balsey, R. Woodman, and J. McClure, "Equatorial spread F: Implications of VHF radar observations," *Journal of Geophysical Research: Space Physics*, vol. 75, no. 34, pp. 7199-7216, 1970, doi: 10.1029/JA075i034p07199.

[7] B. G. Fejer, L. Scherliess, and E. De Paula, "Effects of the vertical plasma drift velocity on the generation and evolution of equatorial spread F," *Journal of Geophysical Research: Space Physics*, vol. 104, no. A9, pp. 19859-19869, 1999, doi: 10.1029/1999ja900271.

[8] S. Tilahun and Y. A. Tariku, "Verification of ionospheric perturbation induced L-band frequency scintillation using HF/VHF bands over the African equatorial and low latitude region, Ethiopia," *Journal of Atmospheric Solar-Terrestrial Physics*, vol. 195, p. 105135, 2019, doi: 10.1016/j.jastp.2019.105135.

[9] A. O. Akala, R. Idolor, F. M. D'ujanga, and P. H. Doherty, "GPS Amplitude Scintillations over Kampala, Uganda, During 2010–2011," *Acta Geophysica*, vol. 64, no. 5, pp. 1903-1915, 2016, doi: 10.1515/acgeo-2016-0052.

[10] N. Wang, L. Guo, Z. Ding, Z. Zhao, Z. Xu, and T. Xu, "The Variation Characteristics of the Spread-F Occurrences at Chongqing in China," in *2018 12th International Symposium on Antennas, Propagation and EM Theory (ISAPE)*, Hangzhou, China, 3-6 Dec. 2018 2018: IEEE, pp. 1-4, doi: 10.1109/ISAPE.2018.8634389.

[11] S. Basu, S. Basu, J. Aarons, J. McClure, and M. Cousins, "On the coexistence of kilometer-and meter-scale irregularities in the nighttime equatorial F region," *Journal of Geophysical Research: Space Physics*, vol. 83, no. A9, pp. 4219-4226, 1978, doi: 10.1029/JA083iA09p04219.

[12] R. Dabas, B. Reddy, D. Lakshmi, and K. Oyama, "Study of anomalous electron temperature variations in the topside ionosphere using HINOTORI satellite data," *Journal of Atmospheric Solar-Terrestrial Physics*, vol. 62, no. 15, pp. 1351-1359, 2000, doi: 10.1016/s1364-6826(00)00126-7

[13] R. Raghavarao and M. Sivaraman, "Ionisation ledges in the equatorial ionosphere," *Nature*, vol. 249, no. 5455, pp. 331-332, 1974, doi: 10.1038/249331a0.

[14] F. M. D'ujanga and S. D. Taabu, "Study on the occurrence characteristics of VHF and L-band ionospheric scintillations over East Africa," *Indian Journal of Radio Space Physics*, vol. 43, no. 4-5, pp. 263-273, 2017, doi: 123456789/29999.

[15] A. D. Gupta and L. Kersley, "Summer daytime scintillation and sporadic-E," *Journal of Atmospheric Solar-Terrestrial Physics*, vol. 38, no. 6, pp. 615-IN2, 1976, doi: 10.1016/0021-9169(76)90157-4.

[16] R. Prasad and S. Kumar, "Day and nighttime L-Band amplitude scintillations during low solar activity at a low latitude station in the South Pacific region," *Journal of Atmospheric and Solar-Terrestrial Physics*, vol. 165, pp. 54-66, 2017, doi: 10.1016/j.jastp.2017.11.005.

[17] D. Zhang *et al.*, "Impact factor for the ionospheric total electron content response to solar flare irradiation," *Journal of Geophysical Research: Space Physics*, vol. 116, no. A4, 2011, doi: 10.1029/2010JA016089.

[18] S. Kumar, A. Kishore, and V. Ramachandran, "Ionospheric scintillations on 3.925 GHz signal from Intelsat (701) at low latitude in the South Pacific region," *Physica Scripta*, vol. 75, no. 3, p. 258, 2007, doi: 10.1088/0031-8949/75/3/005.

[19] B. G. Fejer and M. Kelley, "Ionospheric irregularities," *Reviews of Geophysics*, vol. 18, no. 2, pp. 401-454, 1980, doi: 10.1029/RG018i002p00401.

[20] N. Wang, L. Guo, Z. Zhao, Z. Ding, T. Xu, and S. Sun, "A comparative study of ionospheric spread-F and scintillation at low-and mid-latitudes in China during the 24th solar cycle," *Advances in Space Research*, vol. 63, no. 2, pp. 986-998, 2019, doi: 10.1016/j.asr.2018.10.010.

[21] R. T. Tsunoda, "On seeding equatorial spread F during solstices," *Geophysical Research Letters*, vol. 37, no. 5, 2010, doi: 10.1029/2010GL042576.

[22] B. Forte, S. M. Radicella, and R. G. Ezquer, "A different approach to the analysis of GPS scintillations data," Abdus Salam International Centre for Theoretical Physics, Italy, 2001, vol. 32.

[23] R. Rastogi, P. Koparkar, H. Chandra, and M. Deshpande, "Multifrequency studies of equatorial ionospheric scintillations at Ootacamund," *Journal of atmospheric terrestrial physics*, vol. 52, no. 1, pp. 69-76, 1990, doi: 10.1016/0021-9169(90)90116-5.

[24] M. Abdu, "Outstanding problems in the equatorial ionosphere–thermosphere electrodynamics relevant to spread F," *Journal of Atmospheric and Solar-Terrestrial Physics*, vol. 63, no. 9, pp. 869-884, 2001, doi: 10.1016/S1364-6826(00)00201-7.

[25] P. Ghosh, Y. Otsuka, S. Mani, and H. Shinagawa, "Day-to-day variation of pre-reversal enhancement in the equatorial ionosphere based on GAIA model simulations," *Earth, Planets and Space*, vol. 72, no. 1, pp. 1-8, 2020, doi: 10.1186/s40623-020-01228-9.